

# NAVAL POSTGRADUATE SCHOOL
## Monterey, California




# THESIS

A PRELIMINARY INVESTIGATION OF HIGH AMPLITUDE STANDING WAVES WITH LASER DOPPLER ANEMOMETRY

by

Timothy J. Corrigan

December, 1993

Thesis Advisor: Anthony A. Atchley
Second Reader: D. Felipe Gaitan

Approved for public release; distribution is unlimited.

# REPORT DOCUMENTATION PAGE

Form Approved OMB No. 0704



| 1. AGENCY USE ONLY *(Leave blank)* | 2. REPORT DATE | 3. REPORT TYPE AND DATES COVERED |
|---|---|---|
| | 16November1993. | Master's Thesis |

4. TITLE AND SUBTITLE A PRELIMINARY INVESTIGATION OF HIGH AMPLITUDE STANDING WAVES WITH LASER DOPPLER ANEMOMETRY

5. FUNDING NUMBERS

6. AUTHOR(S) Timothy J. Corrigan

7. PERFORMING ORGANIZATION NAME(S) AND ADDRESS(ES)
Naval Postgraduate School
Monterey CA 93943-5000

8. PERFORMING ORGANIZATION REPORT NUMBER

9. SPONSORING/MONITORING AGENCY NAME(S) AND ADDRESS(ES)

10. SPONSORING/MONITORING AGENCY REPORT NUMBER

11. SUPPLEMENTARY NOTES The views expressed in this thesis are those of the author and do not reflect the official policy or position of the Department of Defense or the U.S. Government.

12a. DISTRIBUTION/AVAILABILITY STATEMENT
Approved for public release; distribution is unlimited.

12b. DISTRIBUTION CODE
A

13. ABSTRACT *(maximum 200 words)*

A previous study of thermoacoustic heat transport phenomena [Atchley et al., J. Acoust. Soc. Am. 88, 251-263 (1990)] reported measurements of the acoustically induced temperature difference $\Delta T$ generated across short, poorly thermally conducting plates situated in high amplitude acoustic standing waves. That study focused on the dependence of $\Delta T$ on the position of the plates in the standing wave, the mean gas pressure and acoustic pressure amplitude. For a given mean gas pressure, there was a threshold acoustic pressure amplitude above which irregularities appeared in the plots of $\Delta T$ vs $kx$. There was evidence that some velocity-dependent effect might be the cause of the discrepancies. An investigation of the acoustic velocity field in high amplitude standing waves has been initiated to determine whether there are measurable irregularities in the velocity field that can account for the observed behavior. The use of Laser Doppler Anemometry (LDA) provided accurate measurements of the velocity behavior of a gas in an empty resonator, as well as in a resonator with a crude thermoacoustic stack. Preliminary results are reported. The major conclusions are that LDA measurements of acoustic velocity fields provide reliable results and there are no significant velocity perturbations evident in our measurements. A videotape of acoustically induced flow in the resonator with a stack indicate that significant velocity perturbations do exist on time scales other than acoustic.

| 14. SUBJECT TERMS Laser Doppler Anemometry; Thermoacoustics | | | 15. NUMBER OF PAGES 54 |
|---|---|---|---|
| | | | 16. PRICE CODE |
| 17. SECURITY CLASSIFICATION OF REPORT Unclassified | 18. SECURITY CLASSIFICATION OF THIS PAGE Unclassified | 19. SECURITY CLASSIFICATION OF ABSTRACT Unclassified | 20. LIMITATION OF ABSTRACT UL |

NSN 7540-01-280-5500 Standard Form 298 (Rev. 2-89)
Prescribed by ANSI Std. 239-18

Approved for public release; distribution is unlimited.

# A PRELIMINARY INVESTIGATION OF HIGH AMPLITUDE STANDING WAVES WITH LASER DOPPLER ANEMOMETRY

by

Timothy J. Corrigan
Lieutenant, United States Navy
B.S., United States Naval Academy, 1987

Submitted in partial fulfillment
of the requirements for the degree of

MASTER OF SCIENCE IN PHYSICS

from the

NAVAL POSTGRADUATE SCHOOL
December 1993

Author: _____
Timothy J. Corrigan

Approved by: _____
Anthony A. Atchley, Thesis Advisor

_____
D. Felipe Gaitan, Second Reader

_____
William B. Colson, Chairman
Department of Physics

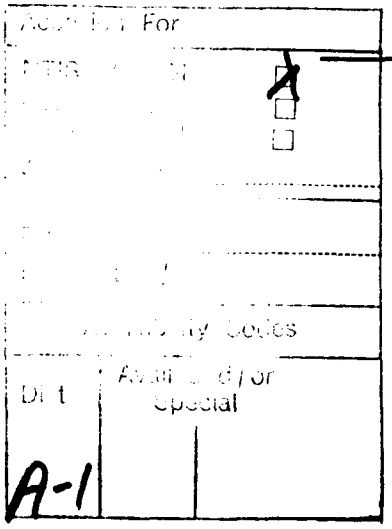

**ABSTRACT**

A previous study of thermoacoustic heat transport phenomena [Atchley et al., J. Acoust. Soc. Am. 88, 251-263 (1990)] reported measurements of the acoustically induced temperature difference $\Delta T$ generated across short, poorly thermally conducting plates situated in high amplitude acoustic standing waves. That study focused on the dependence of $\Delta T$ on the position of the plates in the standing wave, the mean gas pressure and acoustic pressure amplitude. For a given mean gas pressure, there was a threshold acoustic pressure amplitude above which irregularities appeared in the plots of $\Delta T$ vs. $kx$. There was evidence that some velocity-dependent effect might be the cause of the discrepancies. An investigation of the acoustic velocity field in high amplitude standing waves has been initiated to determine whether there measurable irregularities in the velocity field that can account for the observed behavior. The use of Laser Doppler Anemometry (LDA) provided accurate measurements of the velocity behavior of a gas in an empty resonator, as well as in a resonator with a crude thermoacoustic stack. Preliminary results are reported. The major conclusions are that LDA measurements of acoustic velocity fields provide reliable results and there are no significant velocity perturbations evident in our measurements. A videotape of acoustically induced flow in the resonator with a stack indicate that significant velocity perturbations do exist on time scales other than acoustic.

## TABLE OF CONTENTS

## DEDICATION

The list of people to thank for their support in accomplishing this thesis and other degree requirements is long. Although unmentioned, all their contributions are greatly appreciated. First and foremost though, I must thank my wife Terry for her love, patience and support through rough times and many nighttime "deployments" to school. This work, despite not being the first work dedicated to her, is for her. Additionally, I thank my son, Brendan. His blessing of Spanagel Hall has helped all of us reach new levels of inspiration while not riding elevators or eating candy. He and his sister, Kelly (who will not even remember this place), embody true joy, inspiration and love. Thank you's also go to my parents and their many prayers. A quick thanks also goes to true friends, and the runs, racquetball and fish store trips that kept my grades down, but spirits up. Lastly, my lexicon is not wide enough to lay the proper accolades on my advisor, Anthony Atchley. His patience and steady guidance has opened my eyes to a whole, new world I did not know existed two and a half years ago. I view him not just as a friend and advisor, but also somewhat as an oracle.

# I. INTRODUCTION

Thermoacoustic heat transport and its applications, thermoacoustic engines and prime movers, have been examined from various angles over the past decade. The article, "Acoustically generated temperature gradients is short plates" by Atchley, et al [J. Acoust. Soc. Am. **88**, 251-263 (1990)] investigated the acoustically induced temperature difference $\Delta T$ generated across short, poor thermally conducting plates situated in high amplitude acoustic standing waves. In a previous study [Wheatley et al., J. Acoust. Soc. Am. **74**, 153-170 (1983)], and supported by Atchley's study, good agreement between predicted and observed values of $\Delta T$ occurred in low acoustic pressure standing waves (<300 Pa).

The predicted and observed behavior indicated that the $\Delta T$ is a nearly sinusoidal function of its position in the standing wave. Although Wheatley's experiment did not examine standing waves with pressure amplitudes much greater than 300 Pa, he did predict that the sinusoidal behavior would lessen and the pattern would be more saw-tooth in nature. The work by Atchley, et al. approached the higher amplitude standing waves. Although the data did appear more saw-tooth there were discrepancies between the predicted and

measured temperature differences. Specifically, theory and observed results best correlated in the vicinity of the pressure antinode (velocity node). The correlation decreased substantially as the position approached the velocity antinode. This strong evidence that a velocity dependent effect might be the cause of the discrepancies gave motivation to examine the velocity fields in the thermoacoustic resonator.

The goal of this investigation is to examine the velocity fields of high amplitude standing waves in a resonator. The study is conducted primarily by means of Laser Doppler Anemometry (LDA). Results of the investigation give testimony to the viability of this measurement technique. The use of a laser probe and Laser Doppler Anemometry (LDA) allow direct measurement of fluid's velocity in an acoustic standing wave. The results presented are drawn from three scenarios investigated. The first involved measuring the velocity fields in an empty resonator. The data collected is presented in such a manner to examine the field as a function of position in the resonator, as well as providing a relationship between velocity and pressure at their respective antinodes. The second series of experiments involved the emplacement of a crude thermoacoustic stack in the resonator. Data was collected in the immediate vicinity of the edge of the stack to examine the flow properties of the resonator in the

region of the stack. The final trials were conducted by video taping the behavior of the gas aided by the injection of an oil based smoke. Perturbations in the flow behavior of the gas were studied, and the acoustic pressures were noted for any such abnormalities.

## II. EXPERIMENTAL SETUP

### A. THE RESONATOR AND ACOUSTIC DRIVER

To utilize LDA it was necessary to construct a transparent resonator. The resonator was fabricated of 6.45 mm thick plexiglass. A rectangular shape cross section was chosen to provide a flat surface for the laser to penetrate with minimal refraction and distortion. A diagram of the resonator is included in the experimental setup schematic presented in Figure 1. Internally, the resonator measured 100.17 cm long, 5.72 cm wide and 5.08 cm high. A flange and O-ring at the driver end of the tube allowed it to be mounted to a support bracket. The opposing end was closed to provide a rigid boundary. A microphone port was bored into the rigid end. Additionally, two additional ports with aluminum plugs were placed at opposite ends on one of the sides to facilitate to injection of an oil based smoke.

An oil based smoke produced by a ROSCO "fog" generating machine is injected into the resonator prior to taking measurements. The smoke provides particles whose movement in the fluid could be detected by the laser probe. The addition of smoke also facilitates the observation of the

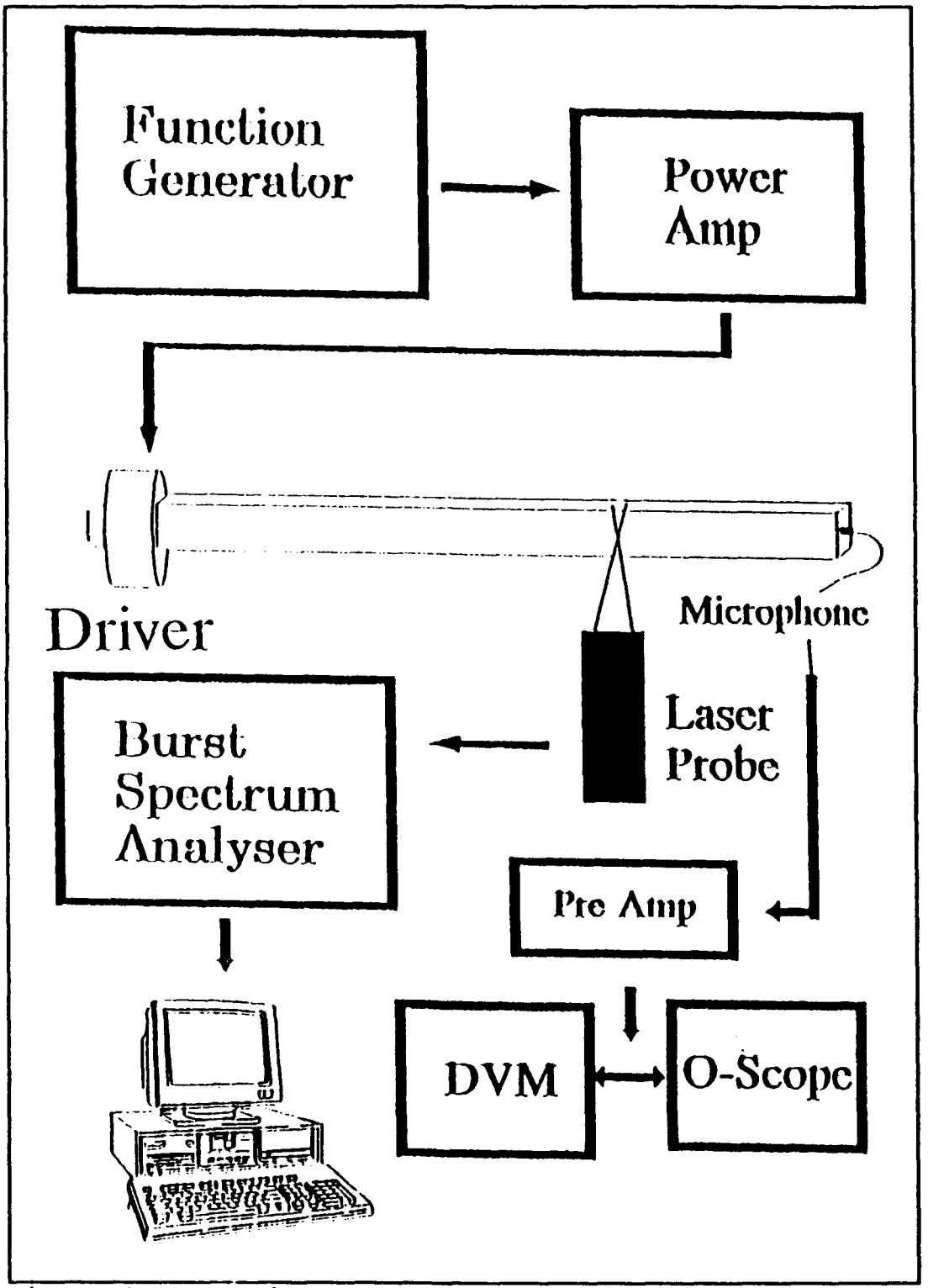


**Figure 1** Schematic of setup used in obtaining LDA data.

gas flow inside the tube. This study assumes that the smoke particles track the motion of the gas inside the resonator. Validation of this assumption is one of the goals of this thesis.

The standing wave needed for these measurements is generated with a JBL compression driver (both models 2445H and 2446J were used) mounted on the same support bracket as the resonator. The throat length of the driver is 5.72 cm, and its diameter is 4.90 cm. The speaker was driven by the output from a Hewlett-Packard 3314A function generator, boosted by a Techron 5530 power supply amplifier.

## B. MEASURING DEVICES

The pressure amplitude of the acoustic standing wave was measured at the rigid end of the resonator. The microphone port housed an Endevco Piezoresistive pressure transducer, model 8510B-5 (S/N 76 mJ). The linear range is 5 psig. The sensitivity of the microphone is 49.72 mV/psi, or 0.00724 mV/Pa. The microphone output was monitored on a Tektronix 2336 oscilloscope and a Hewlett-Packard 3457 digital multimeter after passing through a preamplifier with a gain of 100. The conversion from rms voltage to peak acoustic pressure is given by the following formula:

$$P_{acous} = \frac{\sqrt{2}\ DVM\ (mV)}{sensitivity\ \ Gain}$$

$$= \frac{DVM\ (mV)\sqrt{2}}{0.00724\frac{mV}{Pa}\ (100)}$$

$$= 1.9533\frac{Pa}{mV}\ DVM$$

where *DVM* is the output of the microphone as read by the digital voltage multimeter, *Sensitivity* refers to the microphone's sensitivity, and *Gain* is the gain of the preamp.

One-dimensional velocity measurements were taken by Dantec FiberFlow LDA. The laser is an argon-ion laser. A transmitter takes the beam, separates it by color, splits it, shifts one of the beams by 40 MHz, and launches the beams into an optical fiber manipulator. For these experiments, the green argon-ion line was selected. The two beams are directed by a model 60X10 laser probe. A more detailed description of LDA will follow in the subsequent chapter. The laser probe was mounted on an optical bench that enabled it to be maneuvered along all three axes of the resonator.

Data collection and the subsequent manipulation of that data is controlled by the Dantec 57N10 Burst Spectrum Analyzer (BSA) in conjunction with 486 microcomputer loaded with the Dantec Burstware software package. Burstware enabled the BSA to be controlled from the desktop computer. It also converted the data files so that they could be exported to other software for further processing.

# III. LASER DOPPLER ANEMOMETRY

The primary focus of the investigation is the evaluation of LDA as a reliable measuring tool. This goal is accomplished through measurements of high amplitude standing waves in relatively simple systems. The long term goal is to determine how perturbations in the velocity field affect thermoacoustic heat transport.

LDA is a relatively straightforward technique, and provides an efficient method of non-intrusive flow measurement. Laborious math and physics calculations are involved in spectral analysis, but they are easily handled by the processing hardware and software.

The laser beam used for this study is an argon-ion laser which generates three dominant lines. When fed into the Dantec model 60X40 transmitter, the beam is separated into individual color components. Each color is then split into two beams. The transmitter shifts the frequency of one of the beams by 40 MHz. Two Dantec model 60X24 manipulators connected to the 514.5 nm (green wavelength) output ports couple the beams to polarization preserving, single mode optical fibers. The fibers terminate in the Dantec model 60X10 one-dimensional probe.

The probe is a fiber optical transducer designed for LDA flow measurements in backscatter mode. The two fibers terminate parallel to one another. The front lens of the probe focuses the beams so they cross 160 mm away. The intersection of the beams produces an ellipsoidal measuring volume of 0.0419 $mm^3$. The major axis is 1.77 mm long and the two minor axes are 0.210 and 0.212 mm. Inside the measuring volume, the interference pattern created by the two beams produces a series of 35 fringes 6.0 μm apart.

Due to the 40 MHz shift of one of the beams, the fringes in the measuring volume move along the axis on which the velocity is to be measured. When a stationary particle is in the measuring volume, as shown in Figure 2, the intensity of the of the fringes is focused by the probe lens onto a receiving fiber. This fiber acts as a pinhole section and eliminates reflections from surfaces near the measuring volume. The transmitting and receiving fibers are shielded from each other inside the probe.

Light from the receiving fiber is recollimnated, filtered and sent to a photomultiplier tube. The output of the photomultiplier is represented in Figure 3. This signal is called a "Doppler burst". The time interval between the peaks in the Doppler burst is dependent on the frequency shift of the one beam and the additional shift resulting from the motion of the particle. For the case of the stationary particle, the spacing would give a frequency of

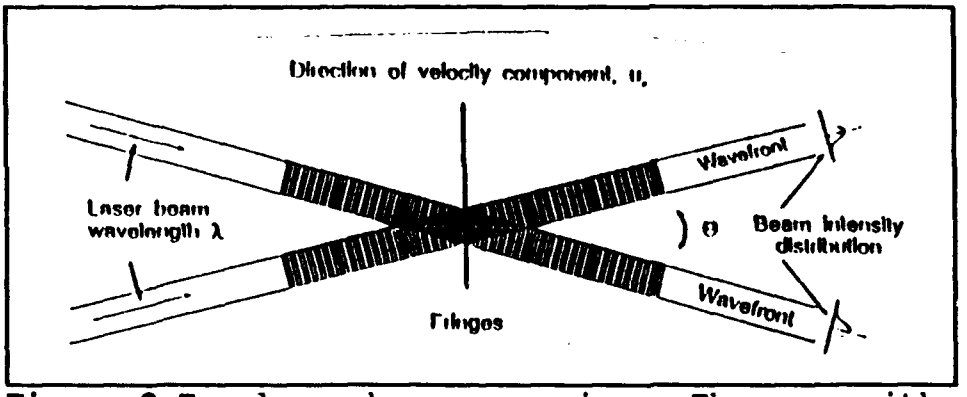


**Figure 2** Two laser beams crossing. The area with the fringes is the measurement volume.

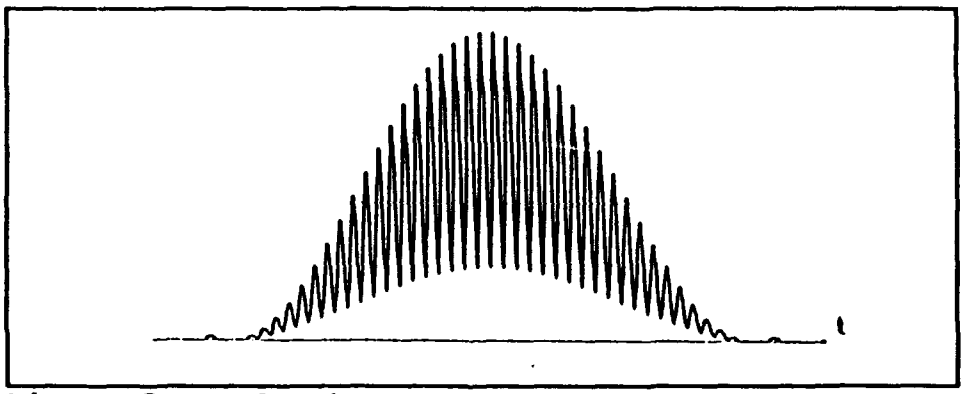

**Figure 3** Doppler burst.

40 MHz. So a frequency of 40 MHz corresponds to a velocity of zero. A particle moving with the fringes would exhibit a larger spacing between the peaks, resulting in a lower frequency, and yield a positive velocity. Negative velocities would result from particles travelling opposite to the fringes' motion.

The Doppler frequency, $f_D$, is calculated by a Discrete Fourier Transform (DFT) of the Doppler burst. With $f_D$, the wavelength of the laser light, $\lambda_L$, and the angle, $\theta$, at which the beams intersect, the velocity of the particle, $u_x$, can be calculated as follows:

$$u_x = f_D \frac{\lambda_L/2}{\sin(\theta/2)} \quad .$$

The velocity measured is the instantaneous velocity of the particle and should therefore be comprised of acoustic, mean and other velocity components of the flow. As discussed earlier, it is assumed that the particle tracks the flow field. Verification of this assumption is one of the goals of this thesis. Up to 16,000 bursts can be evaluated and then plotted by Burstware to depict the velocity field.

# IV. LASER DOPPLER ANEMOMETRY MEASUREMENTS AND RESULTS

## A. EXPERIMENTAL INTRODUCTION

The empty resonator was chosen for the first series of experiments, because it represented the simplest system. A variety of resonance frequencies and acoustic pressures were used to gain an understanding of the relationship between the pressure and velocity fields. We used LDA to measure the velocity waveform, "map" the velocity amplitudes along the axis of the tube, and examine the relationship between the pressure and velocity in the resonator.

The addition of the makeshift stack to the resonator provided a crude model of a thermoacoustic engine. Preliminary measurements were conducted to examine the fluid flow within the vicinity of the leading edge of the stack (the edge closest to the driver).

## B. THE EMPTY RESONATOR

The first sets of measurements were conducted with the empty resonator. Two baseline measurements were made:

1) velocity amplitude vs position in the resonator
2) velocity vs acoustic pressure amplitude at a fixed point.

The procedure used to collect, process, evaluate and display data will only be briefly explained in this section. A more greatly detailed procedural outline is included as Appendix A.

After filling the resonator with smoke, a standing wave is generated. The acoustic pressure is calculated using the DVM reading of the pressure transducer output. The LDA data is processed by the BSA software loaded in the desktop computer. LDA requires that a scattering particle enter the measuring volume to produce a Doppler burst. Since this is a random event, the data rate is unpredictable. To acquire data, the BSA was setup to record 16,000 events. Burstware records (among other things) the velocity and arrival time (relative to the initiation of data acquisition) of the events. It usually requires several seconds to acquire all the data. Hence, data acquisition lasts for thousands of acoustic cycles and the data are taken at random times during the cycle. These data are "folded back" onto a single cycle by recording the arrival time of the sync pulse from the function generator. Knowing the arrival time of the sync pulse allows the arrival time of the Doppler burst to be measured relative to the sync pulse. Hence all the data can be converted to velocity versus arrival time relative to the most recent sync pulse. This operation puts each Doppler burst in the proper phase of the acoustic cycle. The Burstware also converted the data to be further

manipulated by means of a spreadsheet program. The values from the spreadsheet are entered into a graphics program, and the data is fitted by the least squares method shown below:

$$v_{fit} = K0+K1*\sin(K2*at+K3) \ .$$

The velocity offset, *K0*, the fitted amplitude, *K1*, and the phase, *K3*, are calculated from the velocity data, arrival time, *at*, and *K2*. The fixed parameter, *K2*, is obtained by

$$K2 = \frac{2\pi f}{1000} \ .$$

The frequency is divided by 1000 since *at* is in milliseconds. From the fitted curves, velocity amplitudes are obtained. Figure 4 displays data taken at the resonance frequency of 484 Hz at an acoustic pressure of 589.1 Pa. The solid line is the fit to the 3100 data points from the LDA.

The method above was used to generate the velocity amplitudes in Figure 5. The plot is the graph of the velocity amplitude measured at intervals along the center axis of the resonator. The zero of the graph coincides with the rigid end of the tube. The least squares fit shows that the acoustic wave in the resonator is sinusoidal, as would be expected.

The relationship between velocity and pressure in the empty resonator is shown in Figure 6. The velocity was

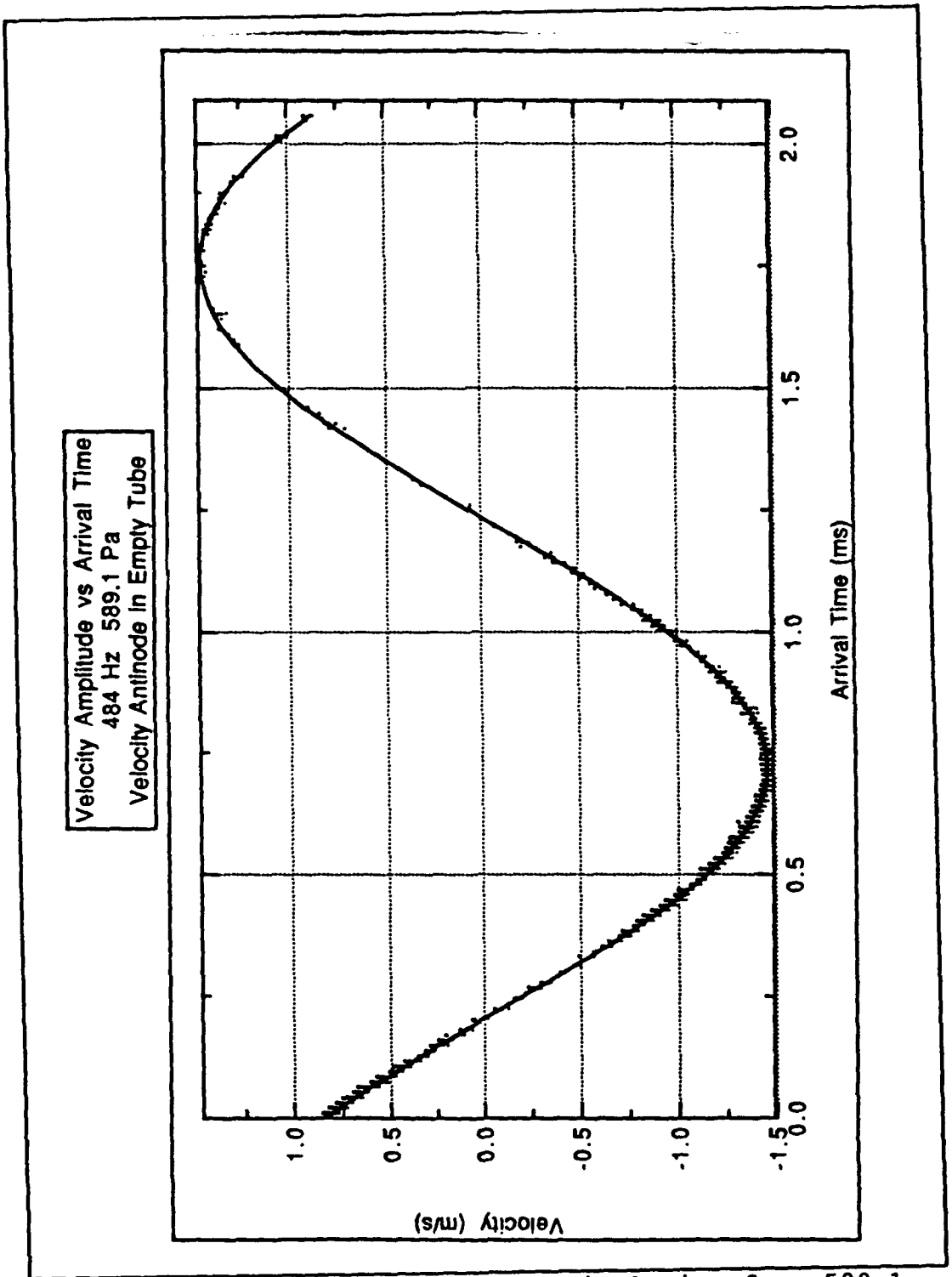


**Figure 4** Graph of velocity vs. arrival time for 589.1 Pa 484 Hz acoustic wave.

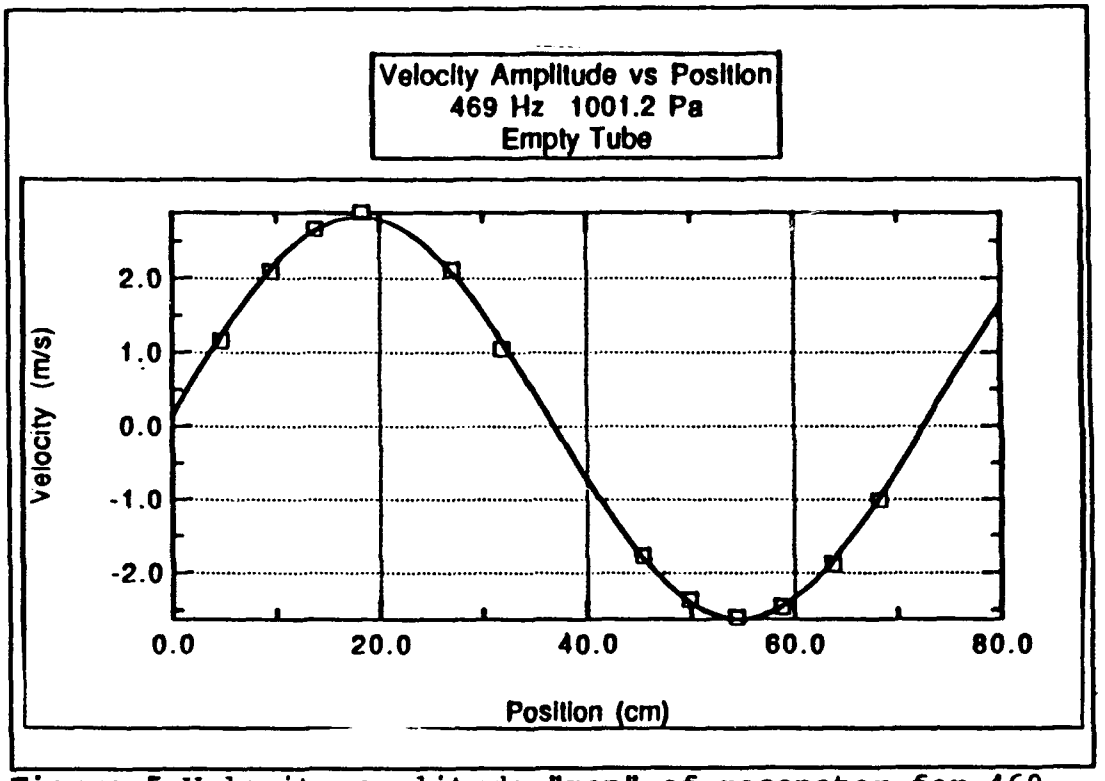


**Figure 5** Velocity amplitude "map" of resonator for 469 Hz.

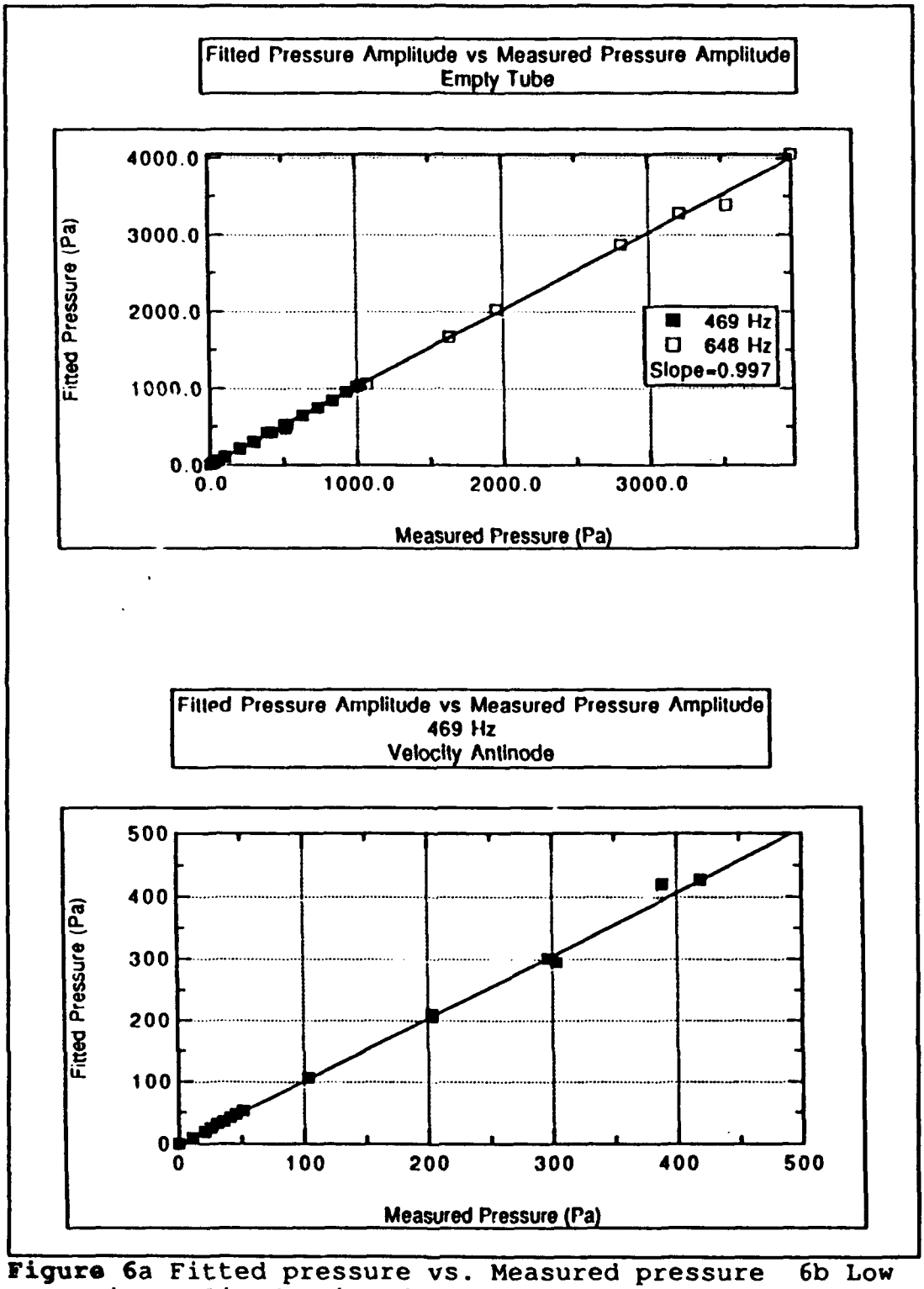


**Figure** 6a Fitted pressure vs. Measured pressure 6b Low acoustic amplitude Fitted pressure vs Measured pressure.

measured at the velocity antinode with LDA. The velocity amplitude was converted to a pressure amplitude by $P=\rho_o cu$ with $\rho_o c$=415 Pa-s/m. The measured pressure was obtained by the microphone housed in the rigid end, allowing the pressure to be measured at the pressure antinode. The plots show the relationship of the fitted pressure to the measured pressure. Even at different frequencies, the fit of the data produces a straight line with a slope of almost unity (0.997). The uncertainty of the measurements fall within the boxes plotted.

The graph of Figure 6b is merely a blow-up of the lower amplitude data of Figure 6a. It is presented along with the top graph to emphasize the range over which these measuring techniques can produce reliable results. The lowest fitted pressure amplitude is 20 Pa, and the range at which data was taken approaches 4000 Pa. There is great confidence that this relationship between the fitted and measured data would exist beyond that range. Measurements at higher amplitudes were precluded due to mechanical limitations of the driver.

The baseline measurements produced three important results. They give confidence in using LDA as a reliable measuring technique. They also help establish that there is nothing unusual or unexpected occurring in the empty resonator. Lastly, the microphone calibration is shown to be accurate.

An interesting result observed from using both pressure and velocity measuring techniques is seen in Figures 7 and 8. Figure 7 shows the overlay of two graphs of data taken at 484 Hz and 589.1 Pa. One is of the fitted velocity curve as a function of time measured at the velocity antinode, and the other is measured pressure as a function of time measured at the pressure antinode. The pressure measurement was recorded by a Nicolet 310 digital oscilloscope. The overlap of the two plots is virtually complete. The wave from the digital oscilloscope was adjusted along the time axis to provide the best overlap. When the voltage to the driver is increased to 3975 Pa, two features are clearly presented, as shown in Figure 8. The waveforms are no longer purely sinusoidal. Both have an increased presence of harmonics, as would be expected. Additionally, the two obviously no longer overlap. The presence of additional harmonics is not beyond what theory predicts for the pressure and velocity waves, but the different shape is a more subtle characteristic and is not a conclusion one would immediately draw.

## C. THE RESONATOR WITH A STACK

To better mimic a thermoacoustic engine, a makeshift stack was built to be placed in the resonator (Figure 9). Fifteen glass microscope slides were cut to size and fitted

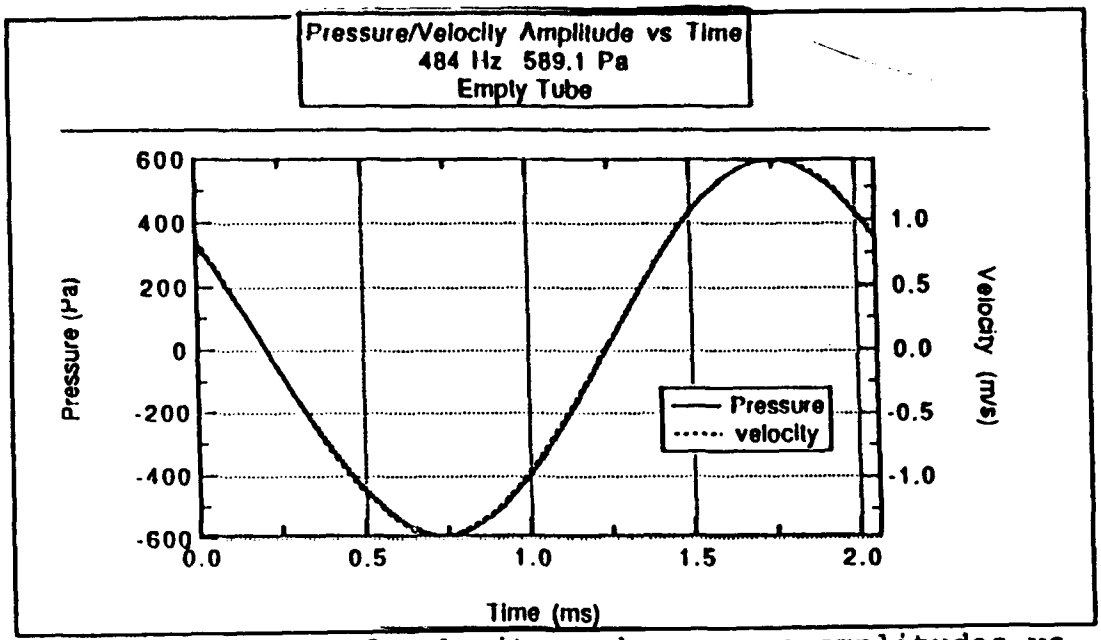


**Figure 7** Overlay of velocity and pressure amplitudes vs. time for low acoustic pressure.

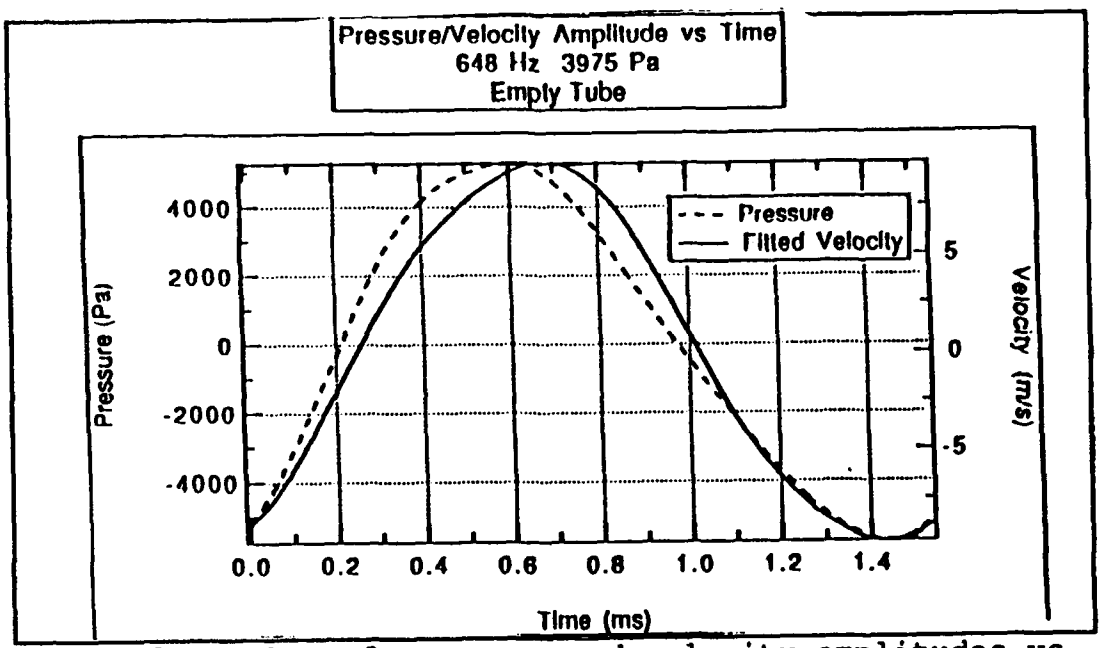


**Figure 8** Overlay of pressure and velocity amplitudes vs. time for high acoustic pressure.

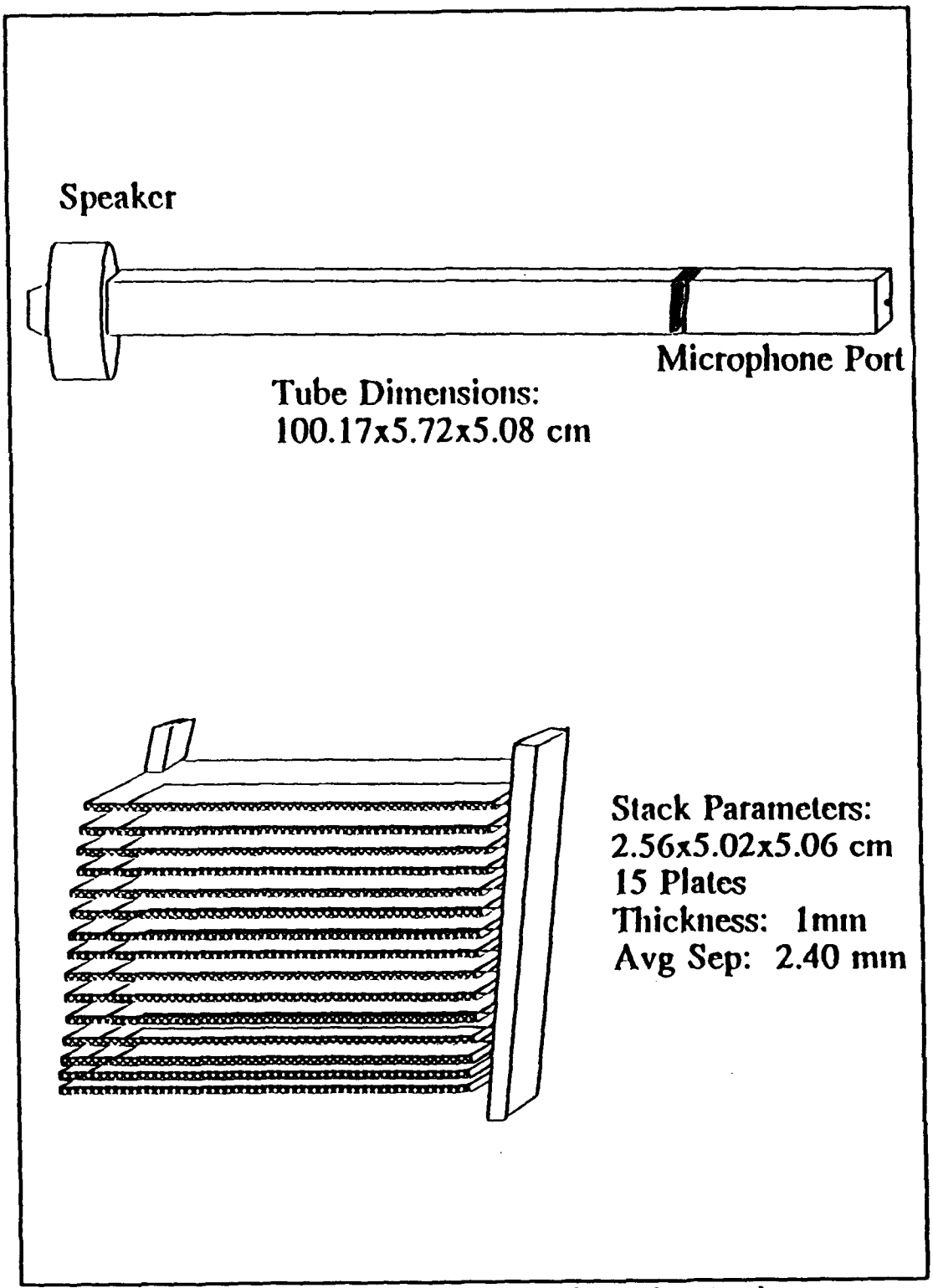


**Figure 9** Schematic of resonator and crude stack.

into two plastic holders and bound with epoxy. The overall stack dimensions (including the slides and holders) measured 2.56 cm long by 5.02 cm wide and 5.06 cm high. The plate thickness is 1.00 mm and the average separation between plates is 2.40 mm. The full listing of stack parameters is included in Appendix B.

The first measurements were taken within the vicinity of the stack to see what types of flow measurements could be taken there. The stack was placed between the velocity node and antinode, the typical placement for a stack in a thermoacoustic engine. The first measurements took data just outside of the stack, on the leading edge and just inside the stack, as shown in Figure 10. Three graphs of the velocity measured at positions relative to the leading edge are presented in Figure 11. All three measurements were made at 1000.7 Pa, as measured by the microphone at the pressure antinode, at 645 Hz. There are no noticeable perturbations in the waveforms, even at higher amplitudes. As the probe measurements entered the stack, the velocity increased, as would be expected from a decrease in cross-section area.

The addition of the stack to the resonator decreased the cross-sectional area of that part of the tube by 29.1%. Figure 12 shows the plot of three sets of velocity amplitudes versus their positions relative to the leading edge of the stack. These three sets of data were recorded

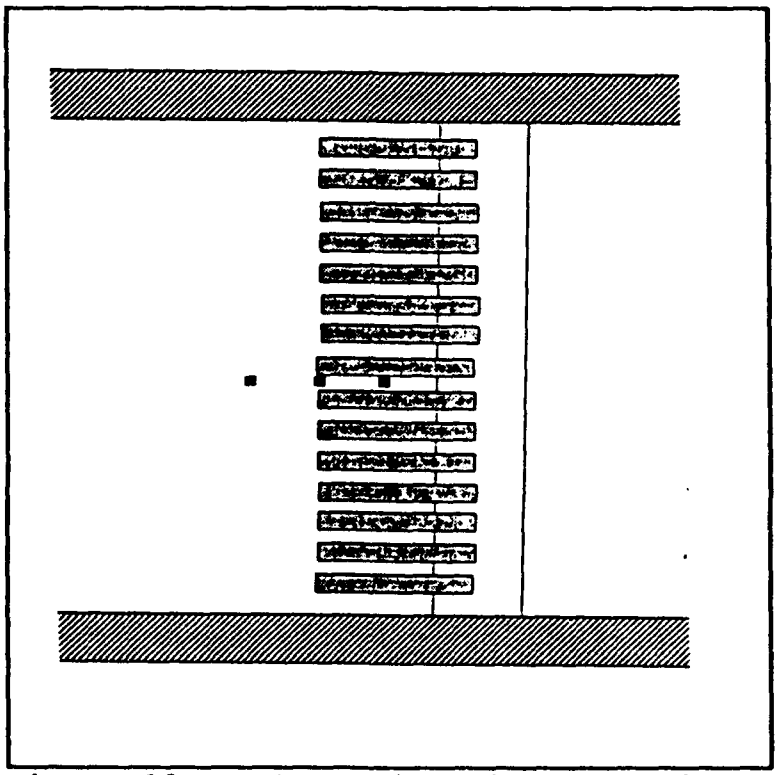

**Figure 10** Stack profile with measuring positions denoted.

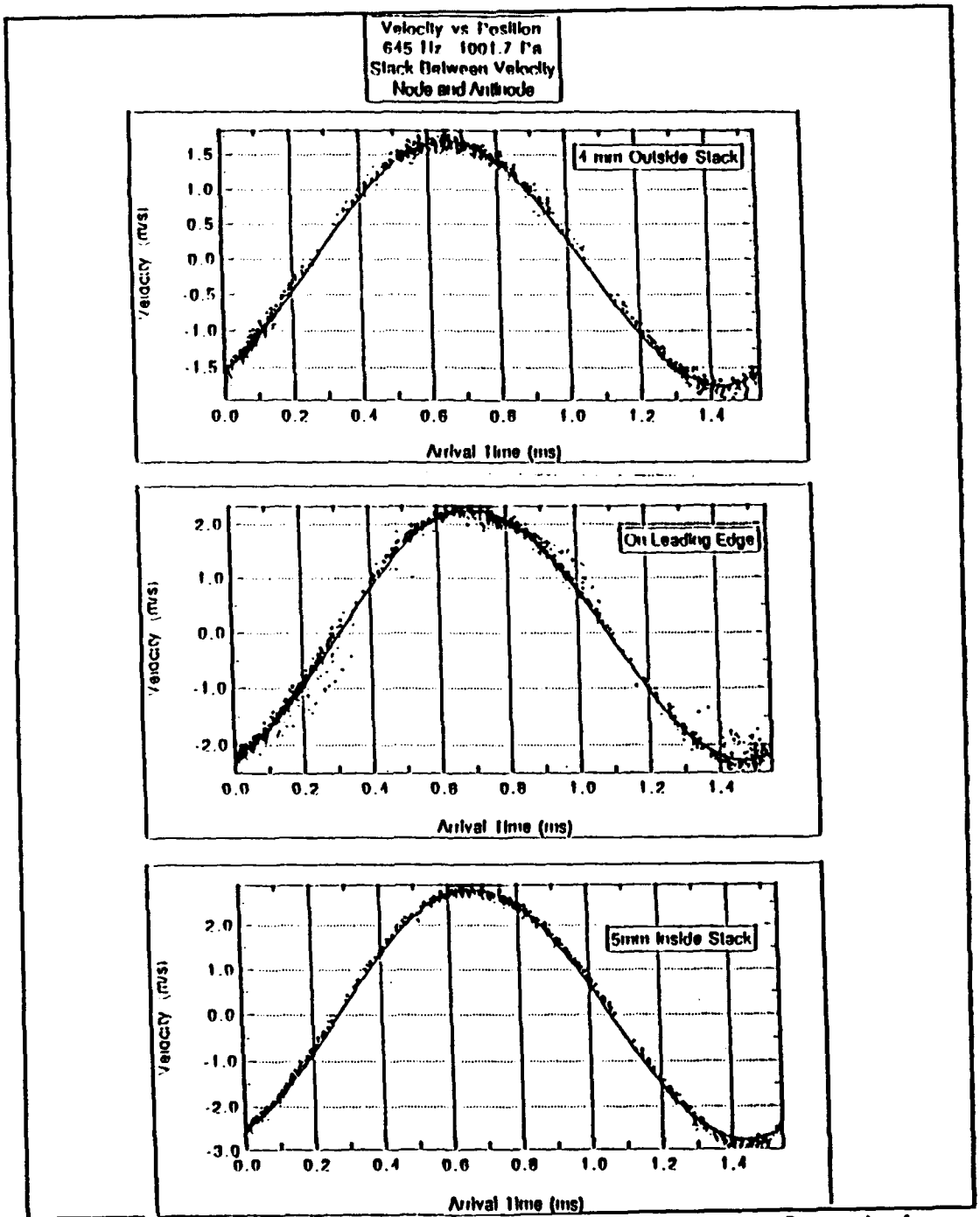


**Figure 11** Velocity vs. position measurements for a) 4 mm outside stack, b) on leading edge, and c) 5 mm inside.

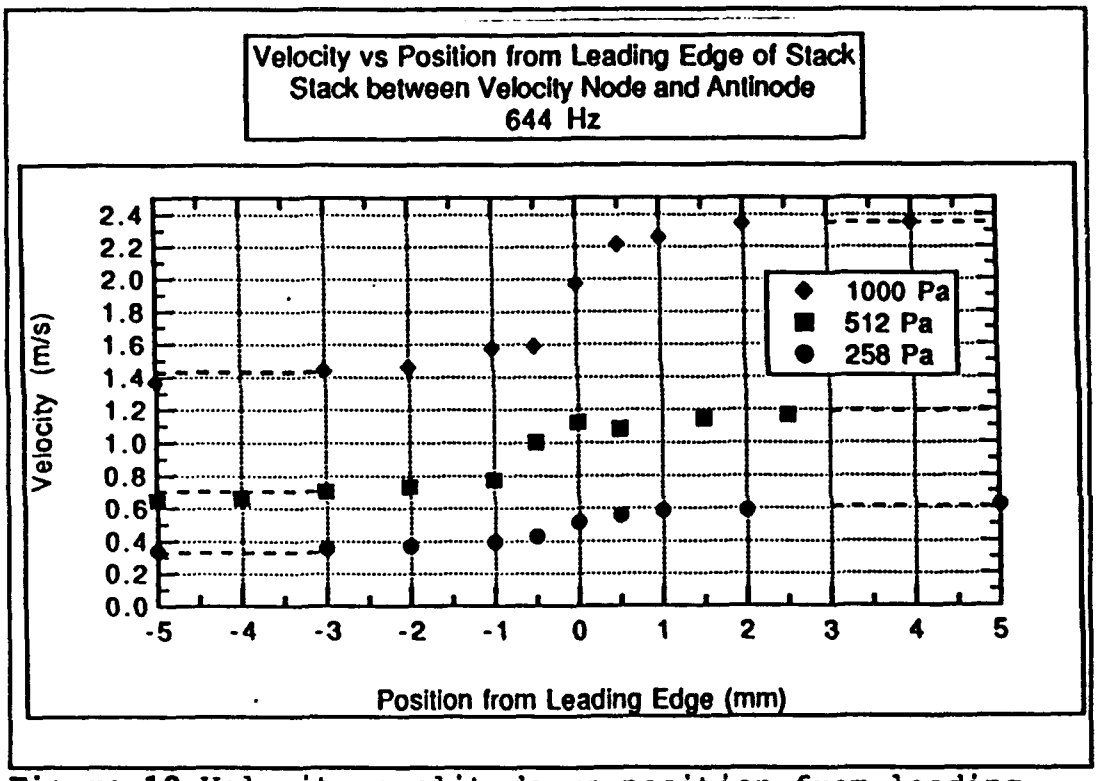


**Figure 12** Velocity amplitude vs position from leading edge of stack.

at different acoustic pressure amplitudes. The dashed lines denote the expected velocity amplitudes for each pressure, taking into account changes in cross-sectional area, and the dependence of velocity on $kx$. When compared to the theoretical values, the fitted velocity amplitude data does not deviate unexpectedly from what would expect in ordinary nozzle flow.

An observation made from the center graph of Figure 11 and from Figure 12 concerns the area just prior to and directly at the leading edge. The scatter of data in the center graph of Figure 11 indicates that there may be some velocity perturbation occurring at the stack's entrance. Figure 12 shows also that the velocity amplitude has increased prior to the decrease in cross-sectional area.

## D. EVALUATION OF LASER DOPPLER ANEMOMETRY

For the simple systems investigated, Laser Doppler Anemometry has shown to be a reliable measuring technique. It performed well over a wide range of acoustic pressures. The velocity versus pressure profile displayed in Figure 6 shows that the velocity amplitudes obtained from the smoke particles do reflect the amplitude of the acoustic flow of the gas. It is still unclear whether the particles are in phase with the gas flow, or whether they lead or lag.

There were some limitations experienced with LDA, however. Due to the dimensions of the measuring volume (order of 100 to 1000 μm) measurements could not be made inside the viscous skin depth (100 μm was largest, down to 85 μm). Also the resonator design did not allow measurements to be made in the regions along the base of the resonator, or too close to the stack plate surfaces.

Since the laser needed the smoke particles to record data, there was a limited number of times smoke could be injected before the tube would have to be cleaned. When the smoke would eventually dissipate, it would start to cloud the plexiglass by forming an oil sheen on the sides. The sheen seemingly made the smoke dissipate faster, causing more build-up. Eventually the laser would not be able to penetrate the film and provide a usable collection of data from the back scatter. The need for smoke also made it too difficult to measure the flow in the regions outside of the stack at high acoustic pressure amplitudes (>1000 Pa), due to the quick dissipation of the smoke.

## V. BEYOND THE NUMBERS--STRANGE FLOW OBSERVATIONS

The results of the trials conducted on both resonator cases have thus far shown that there are no significant velocity perturbations on acoustic time scales in the setup used. The most interesting points surmised from the experiments conducted are how well behaved the flow is in both resonator studies at differing frequencies and acoustic amplitudes. There may, however, be flow behavior at different time scales that could affect heat transport. As a first step toward investigating these processes, a video camera was used to visualize the flow. The next set of investigations gives credence to the wry maxim, "You can observe a lot just by watching." A series of trials were run with both the empty resonator and the resonator containing the stack. After injecting the smoke, the pressure amplitude in the standing wave was increased at varying rates. The behavior of the smoke was noted as a function of acoustic pressure amplitude.

The first effect noticed in the empty resonator was the migration of the smoke towards the pressure antinodes due to radiation pressure. The smoke filled an area that roughly reflected the shape of the standing wave pattern. Figure 13 shows how the smoke (the darkened section of the tube)

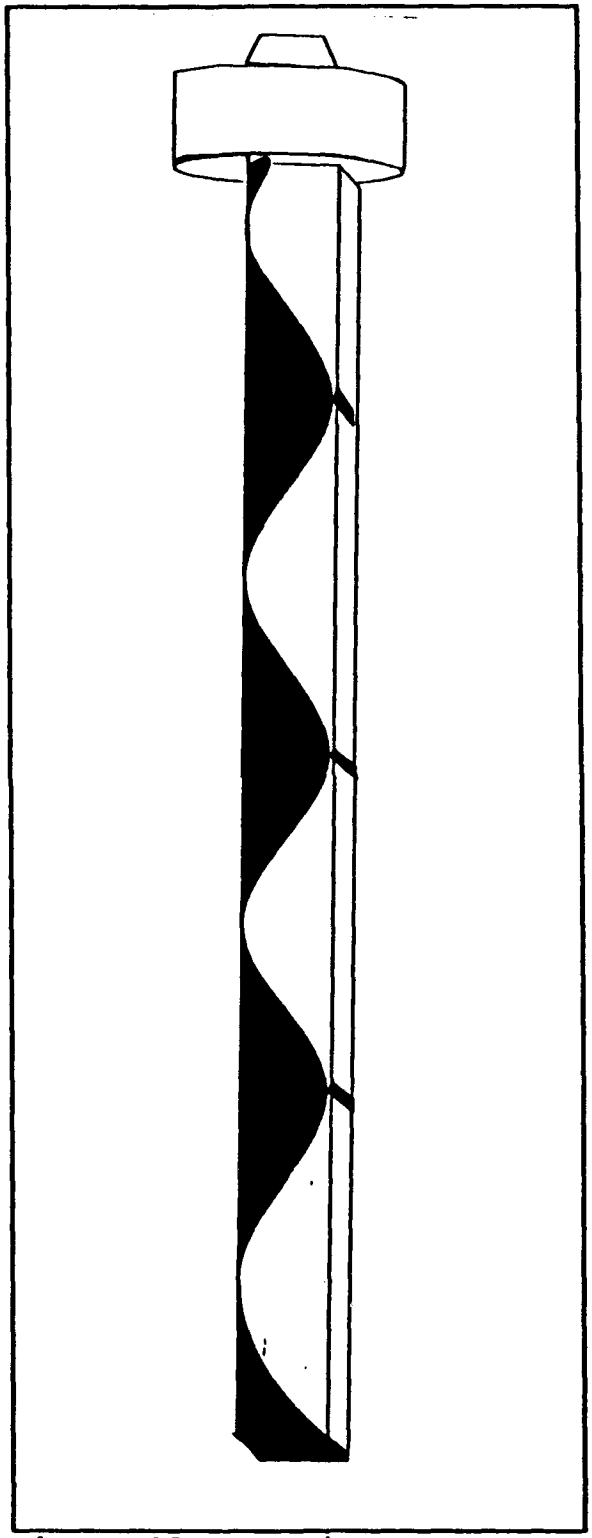

**Figure 13** Smoke in empty resonator.

gathers at the pressure antinodes, indicated by the black strips. As the pressure amplitude is increased more, some of the smoke dissipates, leaving gatherings only at the pressure antinodes. The "life time" of the smoke appears to be related to the acoustic pressure. Eventually, the smoke completely dissipates to the point where it is no longer apparent to the unaided eye. The dissipation is due to the coalescing of smoke particles to the resonator walls. At higher voltages, this coalescence occurs quicker. The smoke at the higher amplitudes behaved as it did in the lower pressure amplitudes, remaining gathered at the pressure antinodes with no aberrations in flow patterns.

Two series of trials were performed on the resonator with the stack. A set of trials were run with the stack placed at the first velocity antinode ($\lambda/4$) from the rigid end. Another set of trials were run with the stack located between the first velocity antinode from the rigid end and the next velocity node toward the driver ($3\lambda/8$ from the rigid end). Similar results were observed from each run.

Generically, when the voltage is first applied to the driver, the smoke gathered at the pressure antinodes as it did in the empty resonator. The increase in velocity of the smoke as it traversed the stack was visible. When the acoustic pressure reached about 450 Pa, a clockwise turbulent flow appeared at the region just past the trailing edge of the stack (the edge farthest from the driver). A

further increase to about 650 Pa caused a similar, but counter-clockwise flow prior to the leading edge of the stack (Figure 14). The turbulent flow was limited to a region approximately one quarter of the acoustic wavelength in size. Even as pressure continued to increase, the regions away from the stack did not show any such behavior. They roughly behaved the same as they did in the empty resonator.

The rate at which the pressure amplitude was increased did not appear to affect the behavior of the flow. The dissipation of smoke occurred more rapidly than it did in the empty resonator. The only difference in behavior noted between the two stack placements involved seeing the first turbulent flow at the trailing edge. Unless the voltage was quickly ramped, the effect could not be seen due to that region be cleared of smoke. With a slow voltage ramp, the clockwise flow could be seen starting at the top quarter of the stack. Again, the effect was only briefly seen as the smoke quickly cleared due to the fast ramping. The second turbulent flow appeared to begin at the bottom quarter of the leading edge, and was easily seen every time, regardless of the voltage ramp speed.

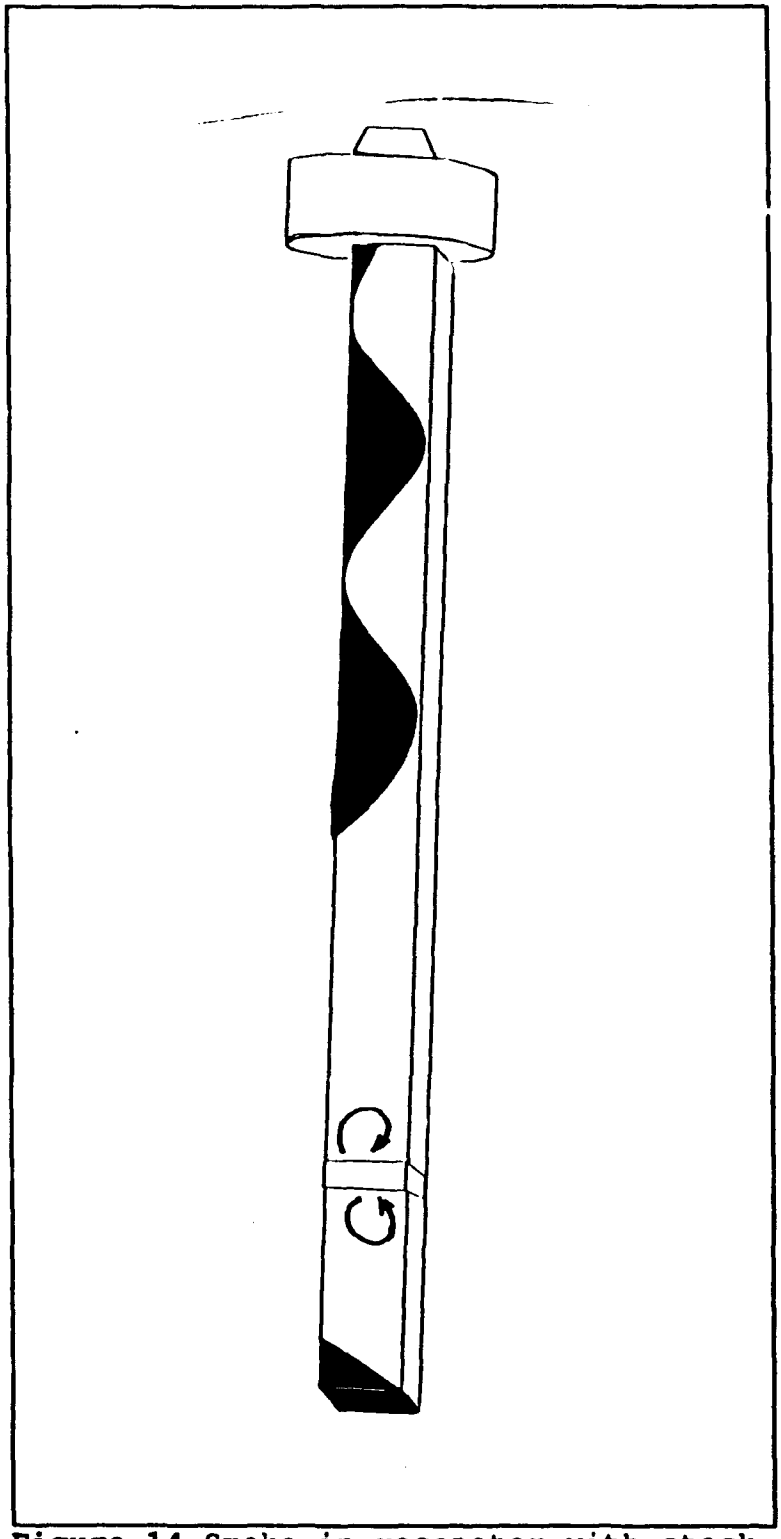

**Figure 14** Smoke in resonator with stack.

# VI. CONCLUSIONS

Several conclusions may be drawn from this work. The velocity versus pressure graph (Figure 6) and the accurate mapping of the resonator by the velocity versus position plot (Figure 5) strongly support the use of Laser Doppler Anemometry as a reliable measuring technique for this type of application. The breadth of uses shown included not only measuring the AC components of the acoustic wave, but also a DC component that could relate to acoustic streaming and other processes. The results obtained also confirm the calibration of the microphone used in measuring the acoustic pressure.

Additionally, it was shown that no significant perturbations of the acoustic velocity occurs over a range of acoustic pressure from 20 Pa to 4000 Pa. The velocity and pressure amplitudes had nearly a one-to-one correspondence over the range examined. The acoustic wave generated by the driver appeared sinusoidal at low pressure amplitudes. The greater presence of harmonics was noted at higher pressure amplitudes. The only subtle characteristic noted was how the pressure and velocity waveforms no longer overlapped at the higher acoustic pressure amplitudes.

The investigation of the velocity in the vicinity of the stack did not reveal any deviant behavior as the fluid flowed through the stack. The velocity increase corresponded to the cross-sectional surface area decrease and the relative proximity to a velocity antinode. The scatter of data within 0.5 mm of the leading edge of the stack may indicates that there may be some type of flow distortion, but no full conclusion can be drawn until further investigation takes place.

The strongest evidence that gives credence to the hypothesis of a velocity-dependent effect occurring in high amplitude standing waves as set forth by Atchley, et al., is the turbulent flow witnessed after a stack is placed inside the resonator. The complex velocity fields observed certainly warrant further investigation. It is additionally worthy to note that the onset of turbulent flow first occurs relatively close to the pressure amplitudes where the irregularities in $\Delta T$ took place in the experiments conducted by the Atchley group. The experimental apparatus and set-up for these experiments could lend themselves with little modification to support further research in examining the flow fields outside of the stack area.

## APPENDIX A-PROCEDURE FOR THE COLLECTION, PROCESSING AND DISPLAY OF LDA DATA

The procedure used for collecting, processing and displaying data used in this thesis will be presented in this section. It should not be assumed that the steps listed are necessarily the only way to achieve results. Similarly, as more and more data is taken, little tricks and short cuts will be discovered that will shorten the process. The steps listed below will show how to measure the acoustic velocity in a standing wave, and fit a curve to the data to obtain a fitted velocity amplitude from an initial setup of the system.

The system consists of the following pieces of equipment:

1. Hewlett-Packard 3314A function generator (FG)
2. Techron 5530 power amplifier
3. JBL 2445H compression driver (speaker)
4. Resonator tube
5. Endevco Piezorestistive transducer, model 8510B-5 (microphone)
6. Preamplifier
7. ROSCO fog generating machine
8. Hewlett-Packard 3457 Digital Voltage Multimeter (DVM)
9. Techtronix 2336 oscilloscope
10. Dantec 57N10 Burst Spectrum Analyzer (BSA)
11. Dantec FiberFlow system consisting of argon-ion laser, 60X40 transmitter, 60X24 manipulator, 60X10 laser probe and other associated equipment
12. IBM compatible 486/33 MHz desktop computer with IEEE card
13. Dantec Burstware software package
14. Dantec "dongle" parallel port key

15. Microsoft Excel
16. Apple MacIntosh desktop computer
17. Igor graphing software package.

The first step would be to turn on all electronic equipment associated with the system. The argon-ion laser and the fog generating machine both require a short warm up period of about five minutes before they can be put into use. The initial disposition of the equipment should be as follows:

1. Function Generator
   a. Sine wave selected
   b. Sync connected to Sync-2 on back side of BSA
   c. Output to channel 1 of oscilloscope and to MONO input of power amp
   d. "free run" mode selected
2. Power Amplifier
   a. Channel 1 control knob in full counter-clockwise position
   b. Output connected to speaker
3. Speaker
   a. Mounted to support bracket
4. Resonator
   a. Mounted to opposite side of support bracket than speaker
   b. Side wall ports plugged
5. Microphone
   a. Housed in microphone port located in end wall of resonator
   b. Connected to preamplifier
6. Preamplifier
   a. Gain set to 100
   b. Output connected to channel 2 of oscilloscope and to DVM
   c. To make a recording of pressure amplitude connect output to a Nicolet digital oscilloscope
7. DVM
   a. Select ACV
8. BSA
   a. Burst mode selected
   b. High voltage set to 1200 V
   c. Local control
9. Dantec FiberFlow system

a. Manipulator connected to green laser line
b. Cap in place on probe
c. FS BNC connector on back of BSA connected to 40 MHz input
d. PM in and PM AUX PWR connectors on back of BSA connected to the photomultiplier tube

10. 486/33 MHz Computer
    a. Dantec dongle connected to parallel interface port
    b. Burstware program running
11. Fog generator
    a. Local control
    b. Fog Volume Control knob set to 10
    c. Green READY light must be illuminated and red HEATER ON light must be off

To obtain a standing wave, a resonance frequency must be found. To do so, select AMPTD on the FG and use the modify knob to get a 1.00 V reading. Turn the power amplifier channel 1 knob clockwise until a sine wave appears on the oscilloscope (actually two will appear). Select the FREQ button on the FG and tune the frequency to get a maximum amplitude on the channel 2 sine wave. That frequency will be the resonance frequency. The poweramp knob can now be returned to its minimum position.

The next series of steps will walk the user through the commands in Burstware necessary to create a file and ready the system to take data.

1. Select SETUP AND ACQUIRE from Burstware menu
2. Select DEVICES
3. Set DEVICE to ENCODER
4. Enable ENCODER
5. Select FILES
6. Select LOAD/SAVE
7. Enter a file name, e.g., TEST
8. Select LOAD
9. Select YES to create TEST.PAR

10. Select ACQUIRE
11. Select QUICK
12. VELOCITY UNITS to m/s
13. CENTER FREQUENCY to 0
14. Enter a BANDWIDTH appropriate to the pressure amplitude to be used. 4.36 MHz is appropriate for most measurements below 1000 Pa.
15. RECORD LENGTH to 32
16. The user will probably want to vary BSA GAIN as necessary. A good rule of thumb is having a GAIN that produces an active SPECTRUM display on the BSA when HIGH VOLTAGE is on.
17. HIGH VOLTAGE to 1200 V
18. MAX ANODE CURRENT to 6.4 mA
19. CYCLE TIME to 100%
20. DEAD TIME to 0 ms
21. SHIFTER MODE to NORM
22. Select OK
23. Select PROG
24. Enter TIME OUT for the maximum length of time desired to record data and NUMBER OF BURSTS for maximum number of bursts desired to collect data. 180 s and 10000 were used often.
25. Select OK

After the laser has warmed, remove the cap from the probe and position the probe at the desired position ensuring the probe is oriented to collect data along the desired axis of the resonator. To fill the resonator with smoke, first remove the two side wall port plugs. Connect the fog generator to one of the ports (a funnel was fabricated to do this). Turn the FOG switch to ON. The smoke can be coaxed through the resonator by attaching a vacuum cleaner hose to the other port. When a dense smoke uniformly fills the resonator, the fog generator and vacuum can be turned off and disconnected, and the plugs returned in place.

To record and process velocity data, the following steps should be followed:

1. Select START from the Burstware ACQUIRE menu (the user should be at this point if the other steps were followed in sequence)
2. Select RUN
3. Select YES to proceed with acquisition.
4. Upon completion of data collection, select OK
5. Select VALID
6. Allow ALL DATA TO OUTPUT BUFFER
7. Select OK
8. Select OK to return to SETUP AND ACQUIRE menu
9. Select the icon with the two "gears" to process the data
10. Select SETUP
11. Select OPTIONS
12. Select ENCODER
13. PULSES PER REVOLUTION to 1, ENCODER ENABLED is YES
14. Select PROCESS
15. Select EXIT
16. Select EXIT
17. Select PRESENT
18. Select SELECT
19. Select ROTATING MACHINERY
20. DISTRIBUTION to TIME BASED
21. DATA TO GRAPH to U VELOCITY
22. MODE to SCATTER
23. FILE TYPE to BEFORE COINCIDENCE FILTER
24. Select OK
25. Select PARAMETER FILE
26. Select TEST.PAR
27. Select DATA FILE
28. Select TESTV0.000
29. Select OK
30. Select DRAW
31. Select ALL
32. Select EXIT
33. SETTING can be used to manipulate the display
34. Select EXIT
35. Select YES to return to the PROCESSING menu
36. Select FILES
37. Select SAVE FILE
38. Select LISTINGS
39. Select PRIM VELOCITY
40. Select BSA1 DATA
41. Select SELECT to select TESTV0.000
42. Select EXPORT
43. Select OK upon completion of conversion to TESTV0.LST

44. Select RETURN to return to main menu
45. Exit Burstware

The data file TESTV0.LST from Burstware contains text and is not formatted properly to be used in Igor. The BSA also puts "dummy" points into the data to help smoothly map out the spectrum. To cull out the non-useable information and leave a file of velocity versus arrival time for one cycle of the acoustic wave velocity measured at the chosen point, Microsoft's Excel spreadsheet program is run. The following is a list of commands to properly format the data for the Igor graphing program.

1. Run Excel
2. Open the TESTV0.LST file created by Burstware
3. Delete the text leaving one empty box just above the numerical data
4. Parse the data into four columns
5. Delete column A, the number corresponding to each sample
6. Now with three columns remaining, delete column B
7. Label the two remaining columns by entering "v" in box A1 for the velocity data and "t" in box B1 for the time data
8. The arrival time for a particular velocity is obtained by adding the corresponding time value to the time value directly preceding it. For box C3, the value would equal box B2 plus box B3. Large blocks of data can be calculated by highlighting the destination blocks (like C3 to C6500) and typing "=B2:B6499+B3:B6500".
9. Upon completion of the calculations, highlight column C
10. Select EDIT
11. Select COPY
12. Select EDIT
13. Select PASTE SPECIAL
14. Select VALUES
15. Label column C "at" in box C1
16. Select column B
17. Select EDIT

18. Select DELETE
19. Select FILE
20. Select SAVE and REPLACE the old TESTV0.LST file
21. Exit Excel and transfer TESTV0.LST to a floppy disk

The graphing program Igor plots data as well as fits the data by the least squares method. After converting and loading the TESTV0.LST file into the Apple MacIntosh (via the Apple File Exchange program), run Igor. One piece of data that should be calculated prior to entering Igor is the wave number for the resonance frequency used divided by 1000. This will be referred to as *K2* in the program and will be used to best fit the data. The next group of instructions will complete the transition from raw data to fitted velocity amplitude.

1. Select FILES, LOAD WAVES, GENERAL TEXT
2. Open the TESTV0.LST file
3. Provide wave names "v" for WAVE0 and "at" for WAVE1
4. At the command line type, "Edit waves v at"
5. Select ANALYSIS, SORTING
6. OPERATION to SORT
7. SOURCE at
8. Select CMD LINE
9. At command line type a space and then, "v at" to sort the data chronologically
10. Select WAVES, MAKE WAVES
11. NAME is VFIT
12. The number of points will be the same number of points contained in v and at
13. Select DO IT
14. At the command line type, "K2=***" where *** will be the calculated value of *K2*
15. Select ANALYSIS, CURVE FITTING
16. CURVE FIT is SIN
17. Select HOLD
18. Select K2
19. YDATA is v
20. XDATA is at
21. DESTINATION is VFIT

22. Select DO IT
23. Select OK upon completion of curve fitting calculations
24. K1 is the fitted velocity amplitude of the LDA data

## APPENDIX B-SPECIFIC PARAMETERS OF THE MAKESHIFT THERMOACOUSTIC STACK

The thermoacoustic stack fabricated for the exploration of velocity fields in high amplitude standing waves was constructed from fifteen glass microscope slides fitted into two plastic holders and bound with epoxy. Figure B1 below is to help facilitate the detailed parameters of the stack.

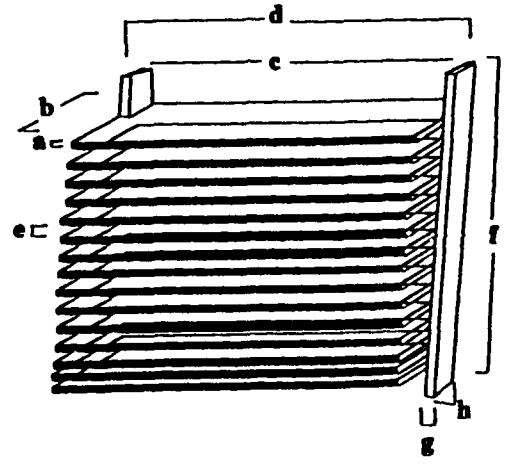


| | | |
|---|---|---|
| a.) | plate thickness: | 1.00 mm |
| b.) | plate length: | 25.60 mm |
| c.) | plate width: | 46.23 mm |
| d.) | overall width: | 50.20 mm |
| e.) | avg. plate sep.: | 2.40 mm |
| f.) | overall height: | 50.62 mm |
| g.) | plastic width: | 4.23 mm |
| h.) | plastic length: | 12.85 mm |

Figure B1 Acoustic stack parameters

The plastic also extends 1.32 mm beyond the edge of the plates and there is 2.73 mm of plastic overlap on the plates. There is 41.76 mm of unobstructed plate width.

The velocity of a fluid is related to the cross-sectional area through which it flows by

$$A_1 V_1 = A_2 V_2 \ .$$

It can be shown that the ratio of velocities outside and inside a stack placed inside a resonator would be

$$\frac{V_2}{V_1} = \frac{1}{1-\frac{A_s}{A_1}} \ .$$

The cross-sectional area of a 5.72 cm by 5.08 cm resonator, $A_1$, would be 29.06 $cm^2$. For the parameters of the stack presented in this appendix, an effective cross-sectional area can be obtained by dividing the stack volume by its length. This would yield a stack cross-sectional area, $A_s$, of 21.65 $cm^2$. By inserting the numbers, it can be shown that $v_2$ is 1.41 times faster than $v_1$.

## LIST OF REFERENCES


1. A.A. Atchley, T.J. Hofler, M.L. Muzzerall, M.D. Kite, and C. Ao, "Acoustically generated temperature gradients in short plates," J. Acoust. Soc. Am. Vol. 88, 251-263 (1990).

2. J. Wheatley, T.J. Hofler, G.W. Swift, and A. Migliori, "An intrinsically irreversible thermoacoustic heat engine," J. Acoust. Soc. Am. Vol. 74, 153-170 (1983).

3. G.W. Swift, "Analysis and performance of a large thermoacoustic engine," J. Acoust. Soc. Am. Vol. 92, 1551-1563 (1992).

4. L.E. Kinsler, A.R. Frey, A.B. Coppens, and J.V. Sanders, "Fundamentals of Acoustics," Third Edition, John Wiley & Sons, Inc., 1982.

5. Dantec Electronik, "User's Guide: 57N10/57N14/57N25 Burst Spectrum Analyzer," Medicinsk og Videnskåbeligt Maleudstyr A/S.

6. Dantec Electronik, "Installation and Reference Manual: 60X FiberFlow Series," Medicinsk og Videnskåbeligt Maleudstyr A/S.

**INITIAL DISTRIBUTION LIST**

| | | No. Copies |
|---|---|---|
| 1. | Defense Technical Information Center<br>Cameron Station<br>Alexandria, VA 22304-6145 | 2 |
| 2. | Library, Code 052<br>Naval Postgraduate School<br>Monterey, CA 93943-5002 | 2 |
| 3. | Prof. Anthony A. Atchley, Code PH/AY<br>Naval Postgraduate School<br>Monterey, CA 93943 | 3 |
| 4. | Prof. D. Felipe Gaitan, Code PH/GN<br>Naval Postgraduate School<br>Monterey, CA 93943 | 1 |
| 5. | Prof. William B. Colson, Code PH/CW<br>Naval Postgraduate School<br>Monterey, CA 93943 | 1 |
| 6. | Dr. Ashok Gopinath<br>Naval Postgraduate School<br>Monterey, CA 93943 | 1 |
| 7. | Dr. Logan E. Hargrove<br>Physics Division--ONR 312<br>800 North Quincy Street<br>Arlington, VA 22217-5660 | 1 |
| 8. | LT Timothy J. Corrigan<br>Box 103<br>9339 Pennywhistle Drive<br>McDaniel, MD 21647 | 2 |
| 9. | Mr. and Mrs. Joseph J. Corrigan<br>Box 103<br>9339 Pennywhistle Drive<br>McDaniel, MD 21647 | 1 |
| 10. | Ms. Rosanne Dovgala<br>1465 Parkside Avenue, Apt. 8-B<br>Trenton, NJ 08638 | 1 |